



# Search for the Eta-Mesic Nucleus From Photo-Production on $^3\text{He}$ in CLAS



## Introduction

The theoretical existence of an attractive force or bound-state between the eta-meson and a nucleon was first discussed by Liu and Haider [1]. A meson is a particle consisting of a quark-antiquark pair, and interacts strongly. From this theory, Chrien et al. [2] expected to see a peak in the momentum of a forward-going proton that correlated to the conditions necessary to produce such an eta; no conclusive evidence was found. It was suggested by Wilkin [3] that this could be due to a broader peak than was expected, and a more efficient way to search for this bound state would be to look for the byproducts of the decay of the eta-mesic nucleus. At Jefferson Lab, we generated eta-mesons by photoproduction on a  $^3\text{He}$  target, and using the data collected in Hall B by the CLAS detector compared our results with the various signatures these and other experiments looked for in hopes of finding conclusive evidence for the existence of this exotic state.

## Motivation

The only meson that has been extensively studied via scattering experiments is the pion, for it is the only meson that has a long enough lifetime to generate a beam; the eta-meson and higher-mass mesons decay too quickly. Therefore, in order to study the eta, we use the nucleus as a laboratory, and generate our eta-beam within the nucleus itself, and have it scatter off of other components of the nucleus. By observing how the eta-meson reacts and scatters within the nucleus, we can learn about the eta, the nucleus, the nucleons within it, and the strong force they use to interact.

## CLAS

The CEBAF Large Acceptance Spectrometer, shown in Figure 1, collected the data used in this experiment. The CEBAF accelerator produced a 2.6 GeV electron beam, which was then converted through a bremsstrahlung tagging system into a photon beam with energies up to 1.5 GeV. The CLAS detector itself consists of six superconducting coils to produce a toroidal magnetic field around the beam axis, with the spaces between the coils filled with start counters to provide event start times, three regions of drift chambers to track charged particles, scintillation counters for time-of-flight measurements, and several other detectors not used in this analysis.

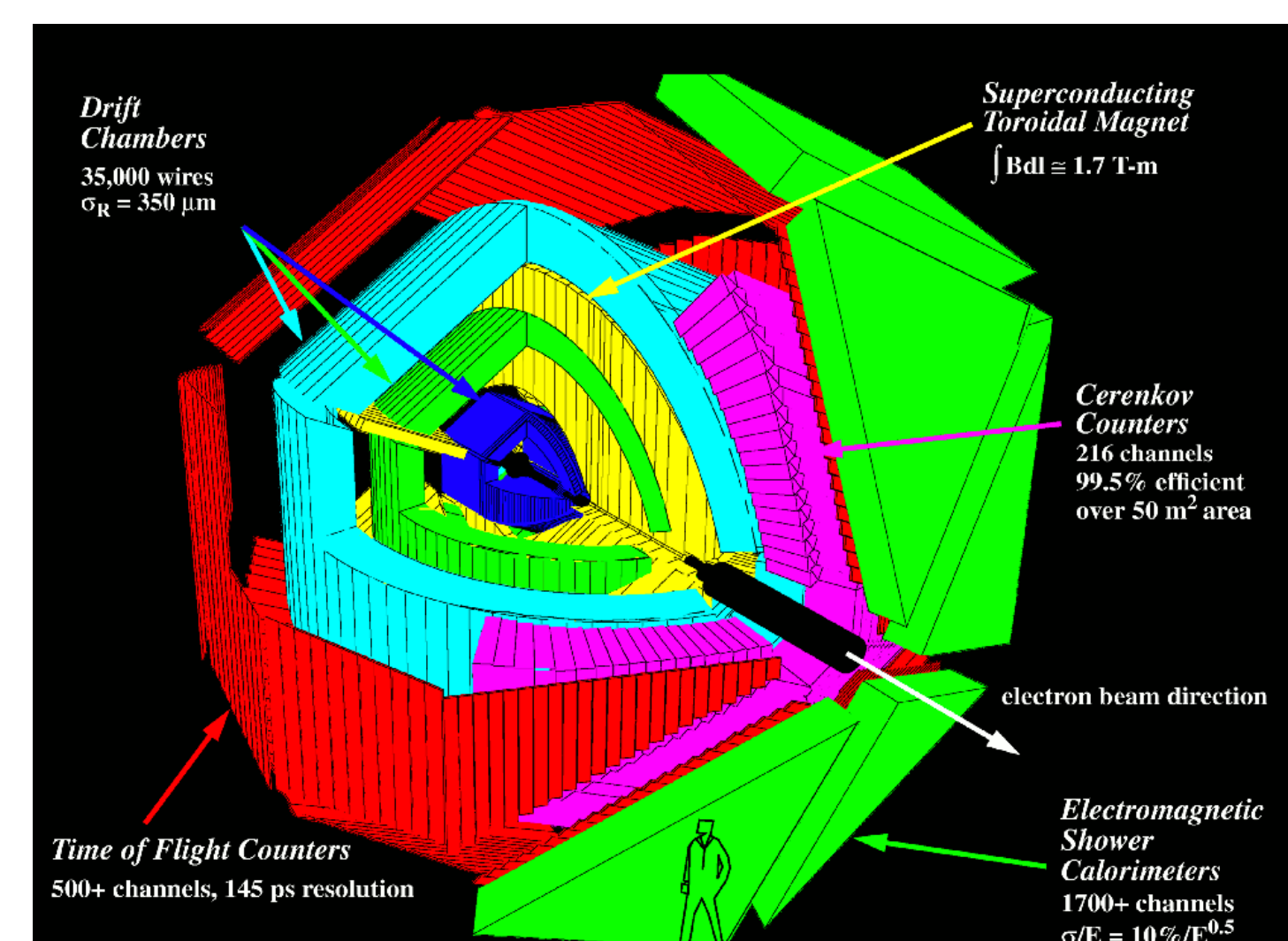


Figure 1: Diagram of the CEBAF Large Acceptance Spectrometer (CLAS) in Hall B at Jefferson Lab.

## Predicted Process

To produce an eta-meson, we bombarded a liquid  $^3\text{He}$  target with photons, exciting the nucleons within. When this first excited state decayed, some eta-mesons were produced. If this eta had low enough momentum, it could have been captured by another nucleon to form a short-lived bound state, the eta-mesic nucleus. When this resonance collapsed, the second nucleon became excited, and it soon decayed. Since the eta had low momentum, and the nucleon was almost at rest, the products of this second decay must scatter back-to-back from each other in order to conserve momentum. Figure 2 displays an example of this behavior, where a proton and neutron are excited, and the eta-mesic nucleus decays via pion emission.

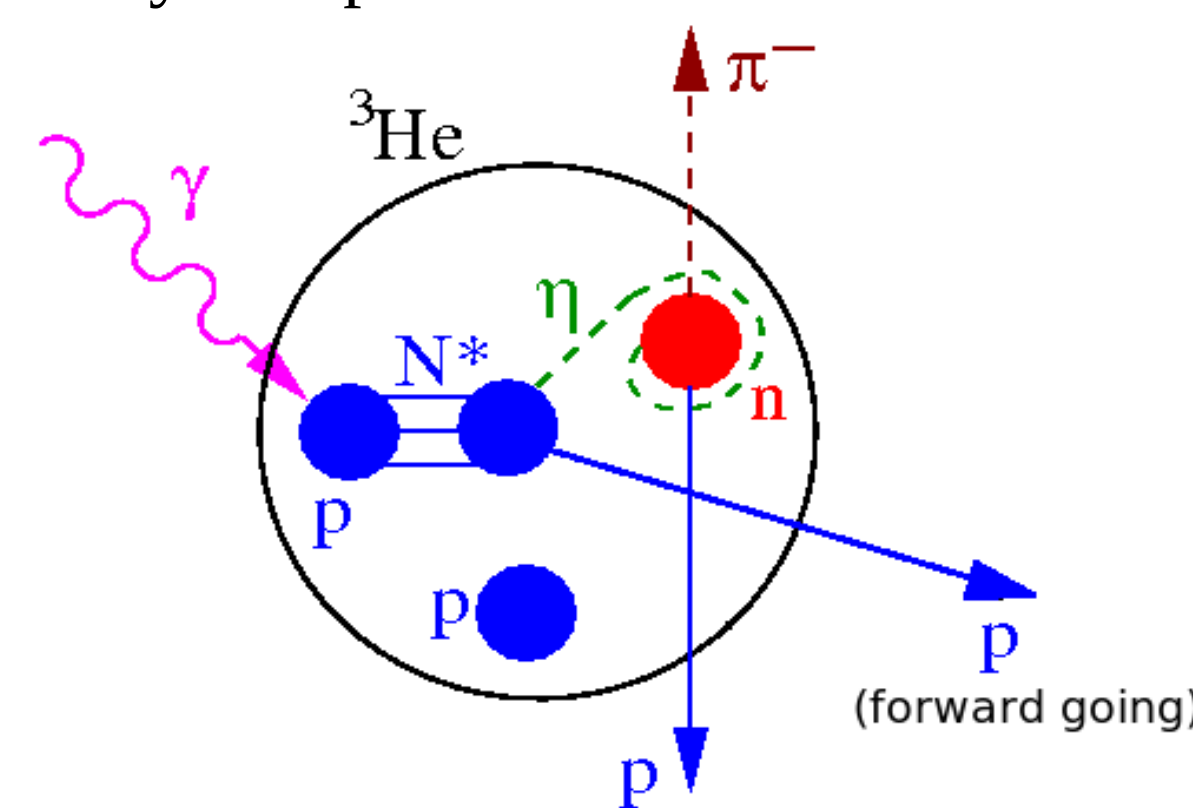


Figure 2: An example of a reaction forming an eta-mesic nucleus in  $^3\text{He}$ , including reaction products.

## Data Analysis

In order to cut out background events, where an eta-mesic nucleus cannot be formed, a series of cuts on the data were used. The first involved determining which photon from the tagger created the event within CLAS. This was done by putting a cut on the difference between the tagger-time and the start-counter event time. Figure 3 shows a histogram of tagger time minus event time. The red lines indicate these cuts.

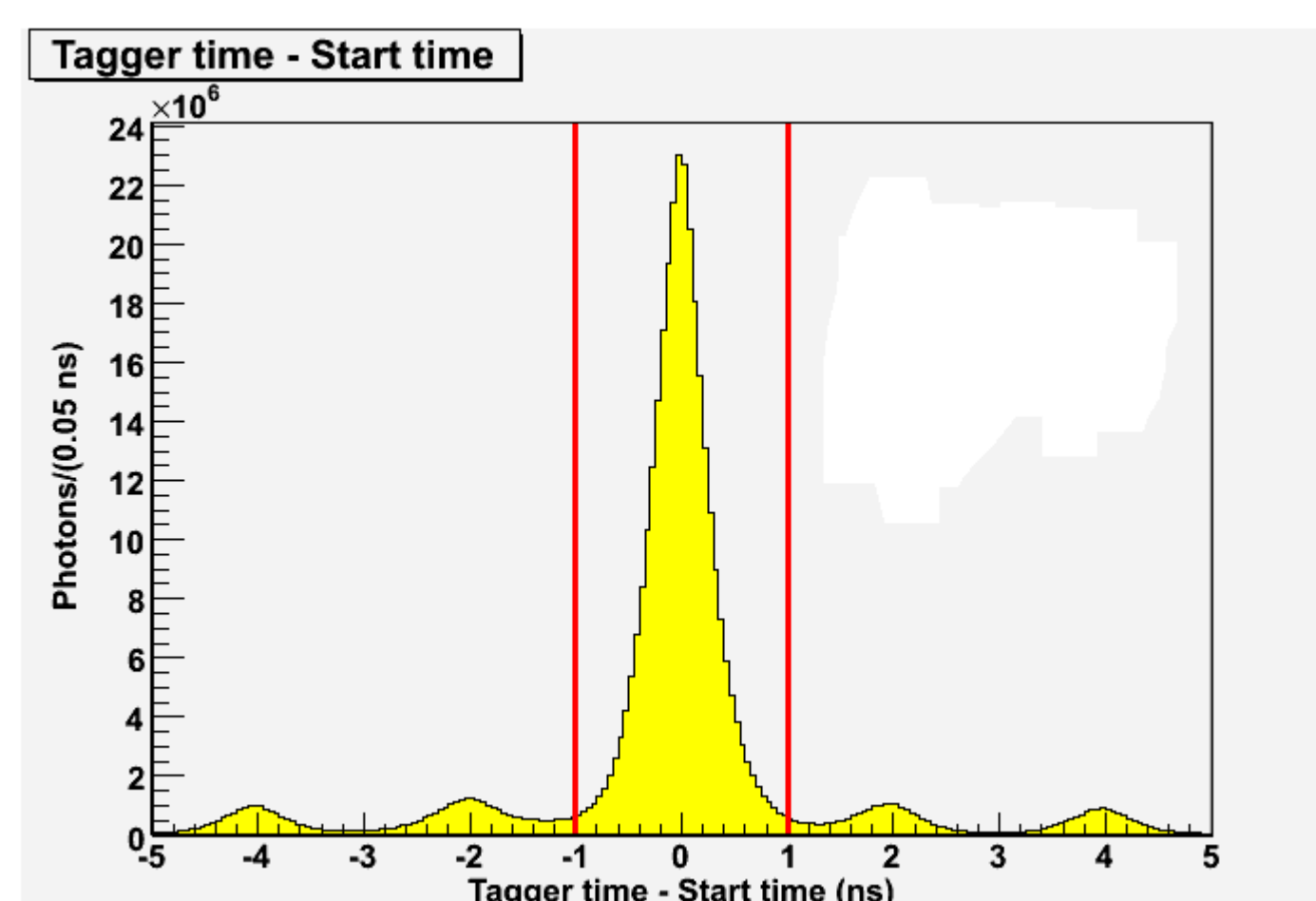


Figure 3: Histogram of tagger time minus start time for all incident photons. The red lines indicate cuts for determining photons with good coincidence.

## Identifying Particles

While running through all of the events, it is necessary to identify and tag each event and each particle in the event. The momentum and trajectories of charged particle are measured by the drift chambers as they move through the magnetic field; the time-of-flight scintillators measure the velocity of the particles. By graphing  $\beta$  ( $v/c$ ) as a function of momentum, clear particle differentiation occurs. The red boxes show the cuts we used to identify protons and  $\pi^+$

Peter Bonventre and Michael F. Vineyard  
Department of Physics and Astronomy  
(The CLAS Collaboration)

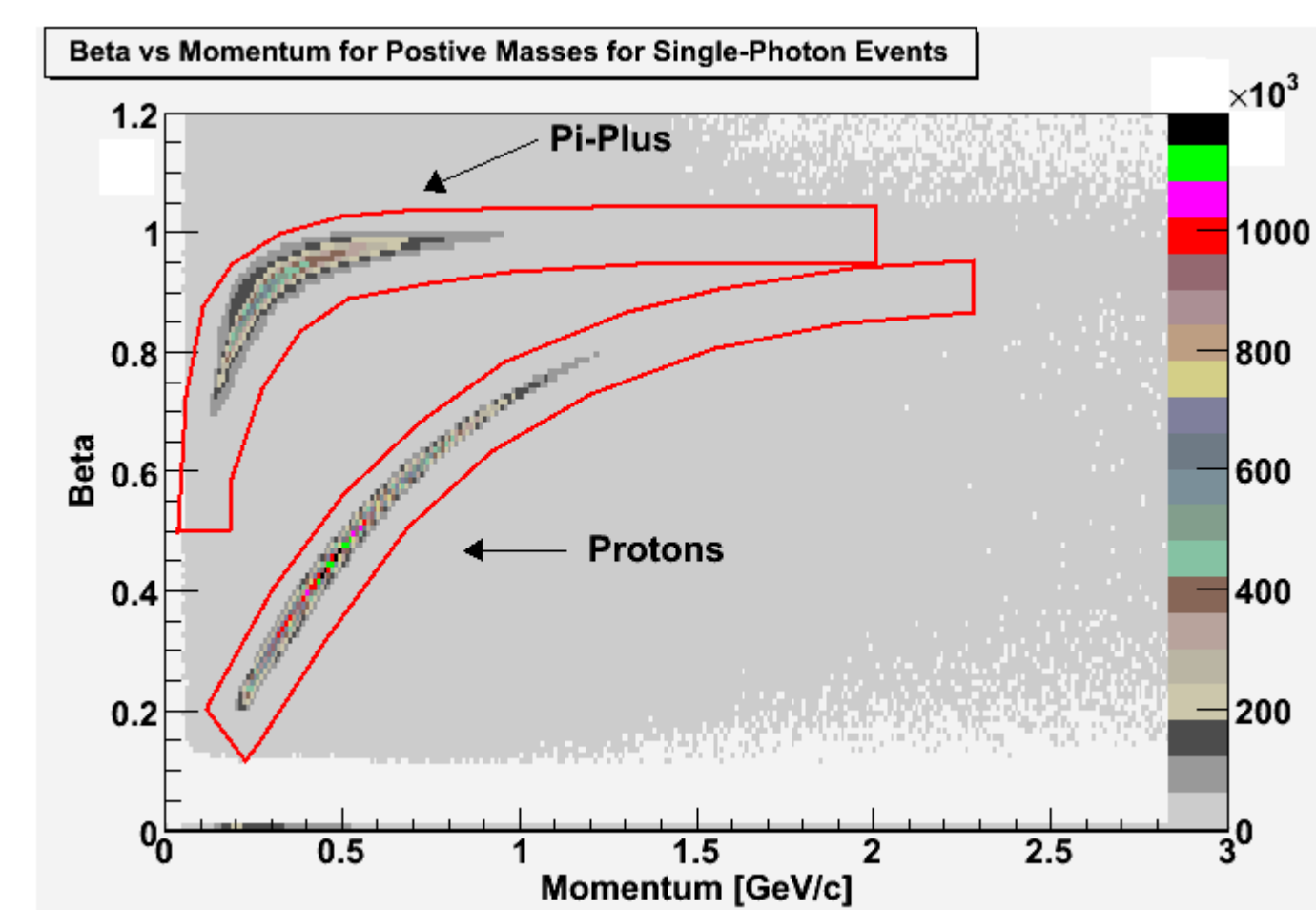


Figure 4: Histogram for beta vs momentum for positive particles. The red lines indicate cuts applied to identify pions and protons.

## Corrections and Cuts

Once particles were identified, fiducial cuts were applied to define regions of the detectors with uniform efficiency, and momentum corrections were applied to correct for energy losses as the particles moved through the detector. We further reduced our volume of events by only looking at specific three-particle coincidences: a forward-going proton (with an angle of less than  $25^\circ$  from the photon beam) occurring with another proton and  $\pi^-$ . These last two particles represent a specific decay mode of the collapsed eta-mesic nucleus, as shown in Figure 2. In order to conserve the small momentum found in the eta-mesic nucleus, these two particles must be produced back-to-back to each other, with angles between  $160$  and  $180$ . These cuts formed a specific volume of data to be analyzed.

## Momentum Peak

Theoretical studies [1] suggested that a possible signature for the eta-mesic nucleus would be a peak in the momentum spectrum of the forward-going proton. Figure 4 shows three momentum distributions for the forward-going proton in coincidence with a back-to-back proton and  $\pi^-$  events. Each distribution corresponds to a different range in incident photon energy. Note that we see no significant extra peaks, nor any major difference between the various distributions.

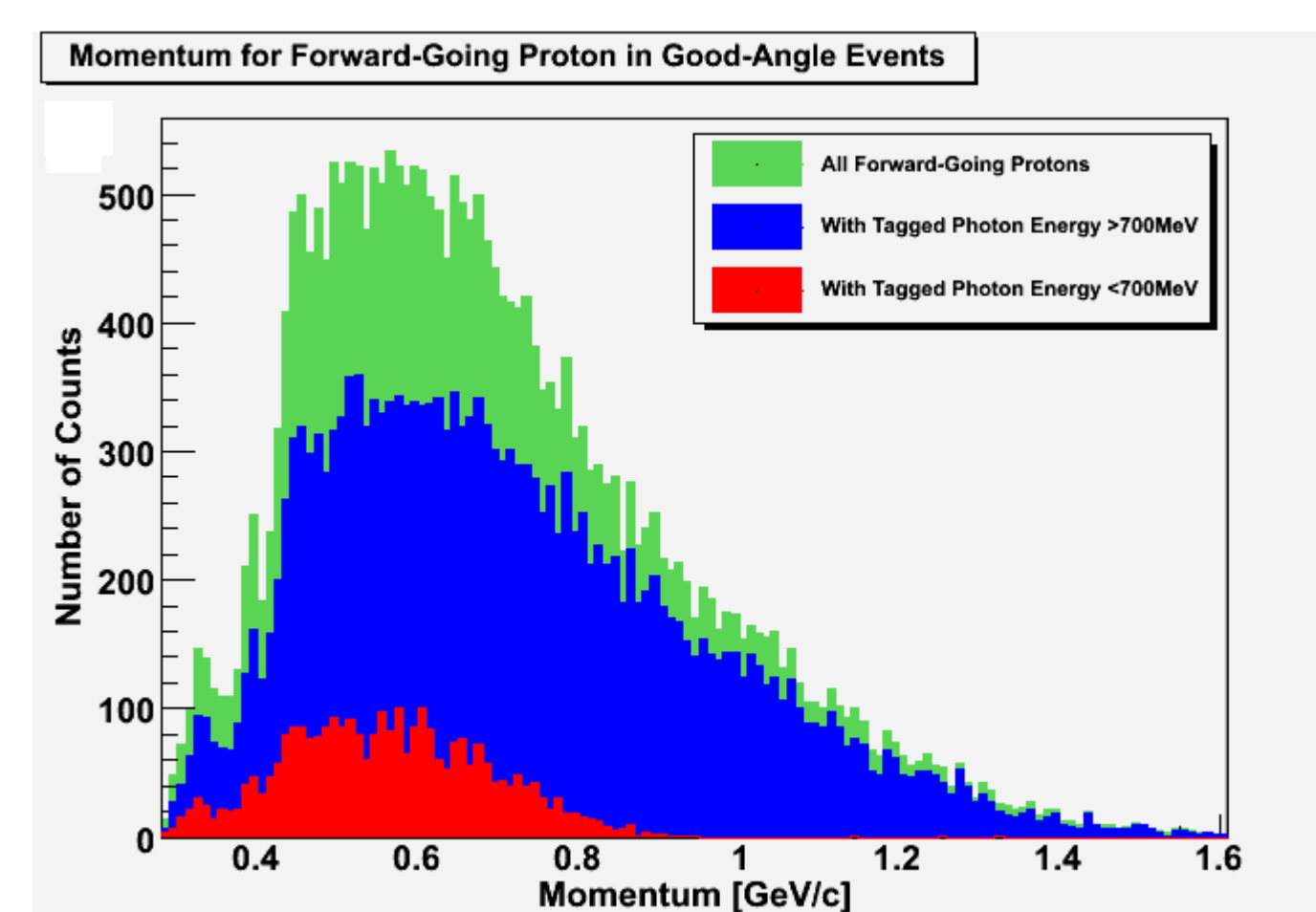


Figure 5: Momentum distributions for the forward-going proton in coincidence with back-to-back proton and  $\pi^-$ .

## Invariant Mass

While no major peak was observed in the momentum spectrum, we followed up with method suggested by Pfeiffer [4]. He suggested that a peak would form in the graph of the invariant mass of the decay products of the bound-state at the energy of the excited state of the nucleon where eta-mesons can be produced, or  $S_{11}$  (1535 MeV). Figure 6 compares the invariant mass displays of the back-to-back proton and  $\pi^-$  at different tagged photon energies, with the blues above 650 MeV and the reds below. Both peaks seen in each graph represent the overlapping peaks of the various excited states of the proton; the first is mostly dominated by the  $\Delta(1232)$ , which cannot produce eta-mesons, while the second has no definite singular component. While we expected a strong  $S_{11}$  peak, we do not see one above the background.

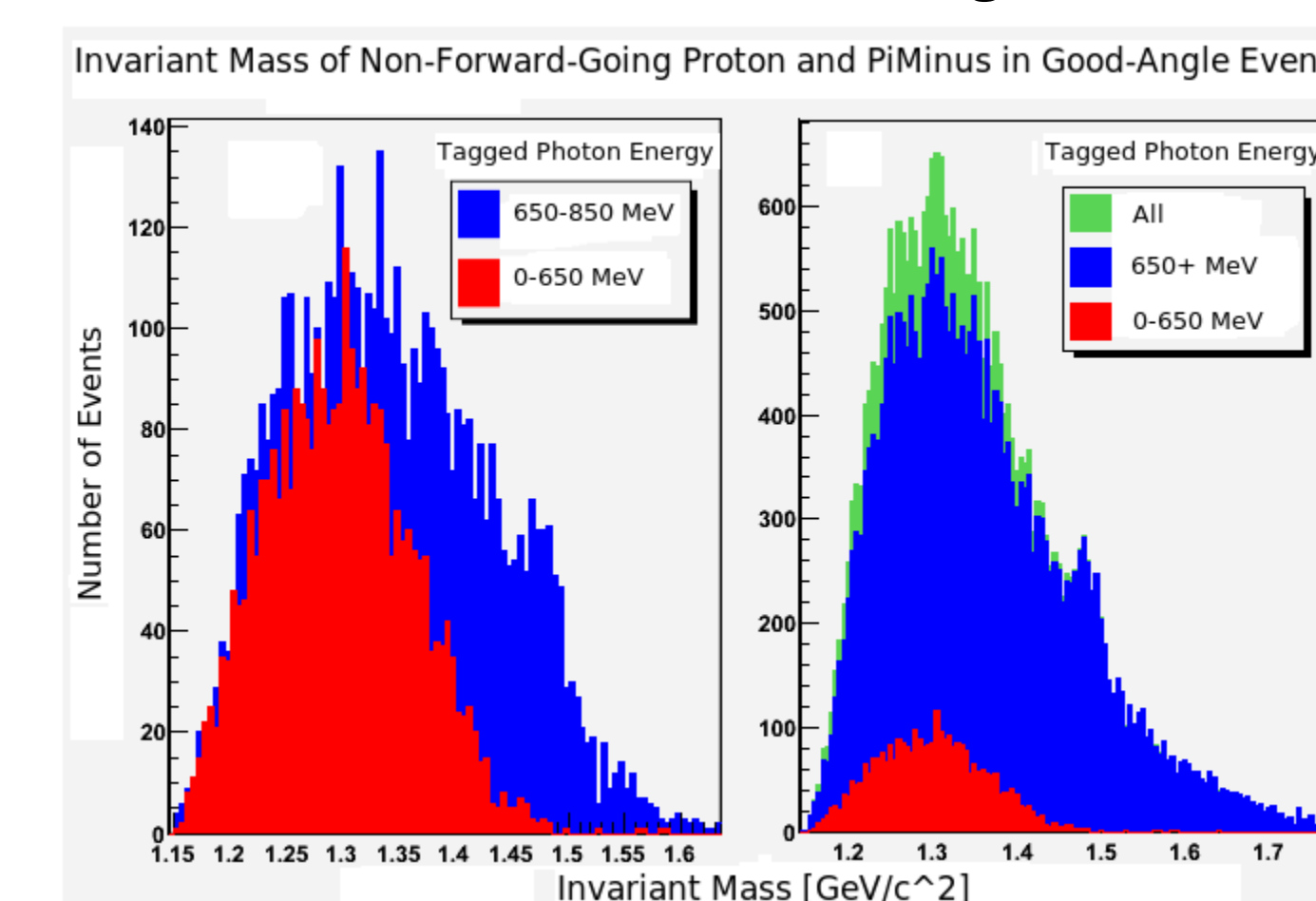


Figure 6a and 6b: The invariant mass spectra of the back-to-back proton and  $\pi^-$ .

## Scaled Subtraction

Pfeiffer also used a different method of exploiting the invariant masses of the back-to-back particles. He looked at how the graphs of the invariant mass changed when looking at angles in the  $150$ - $170^\circ$  range as compared with the  $170$ - $180^\circ$  range. He scaled and normalized the two graphs, and subtracted the difference. However, in our data, presented in Figure 7, the two peaks do not line up, and in fact have very different shapes, so subtraction and normalization was not possible, nor would it generate the same effect Pfeiffer was looking for.

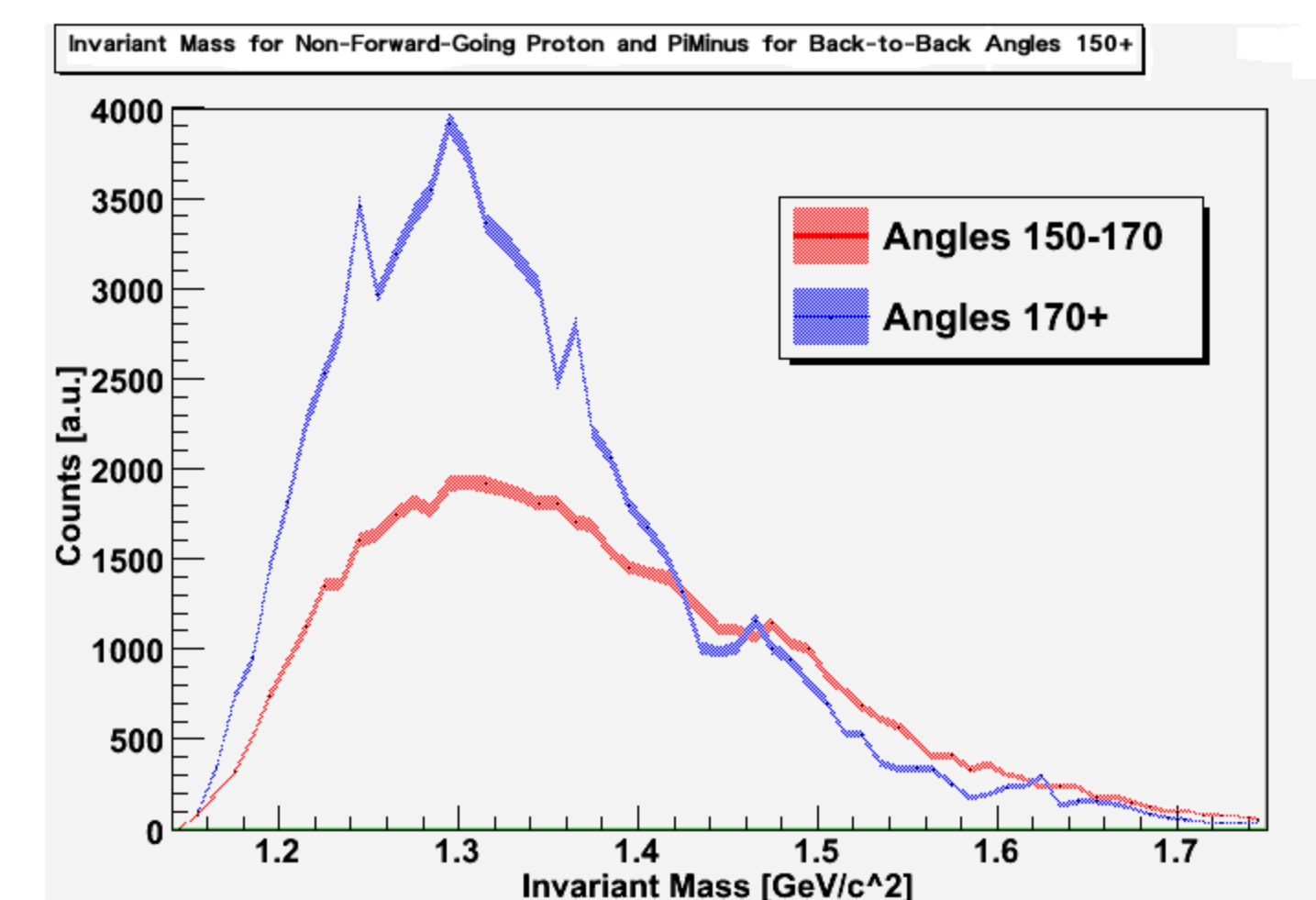


Figure 7: Invariant mass distributions for back-to-back proton and  $\pi^-$  based on the angle between them.

## Kinetic Energy

Another collaboration, Sokol [5] and Baskov et al. [6], saw differences in the peaks in the two-dimensional histograms comparing the kinetic energy of the  $\pi^-$  against the total kinetic energy of the back-to-back proton- $\pi^-$  system, when viewed below the eta-production threshold and then above it. We plotted this comparison in Figure 8; however, it does not show the structure suggested by Sokol et al.

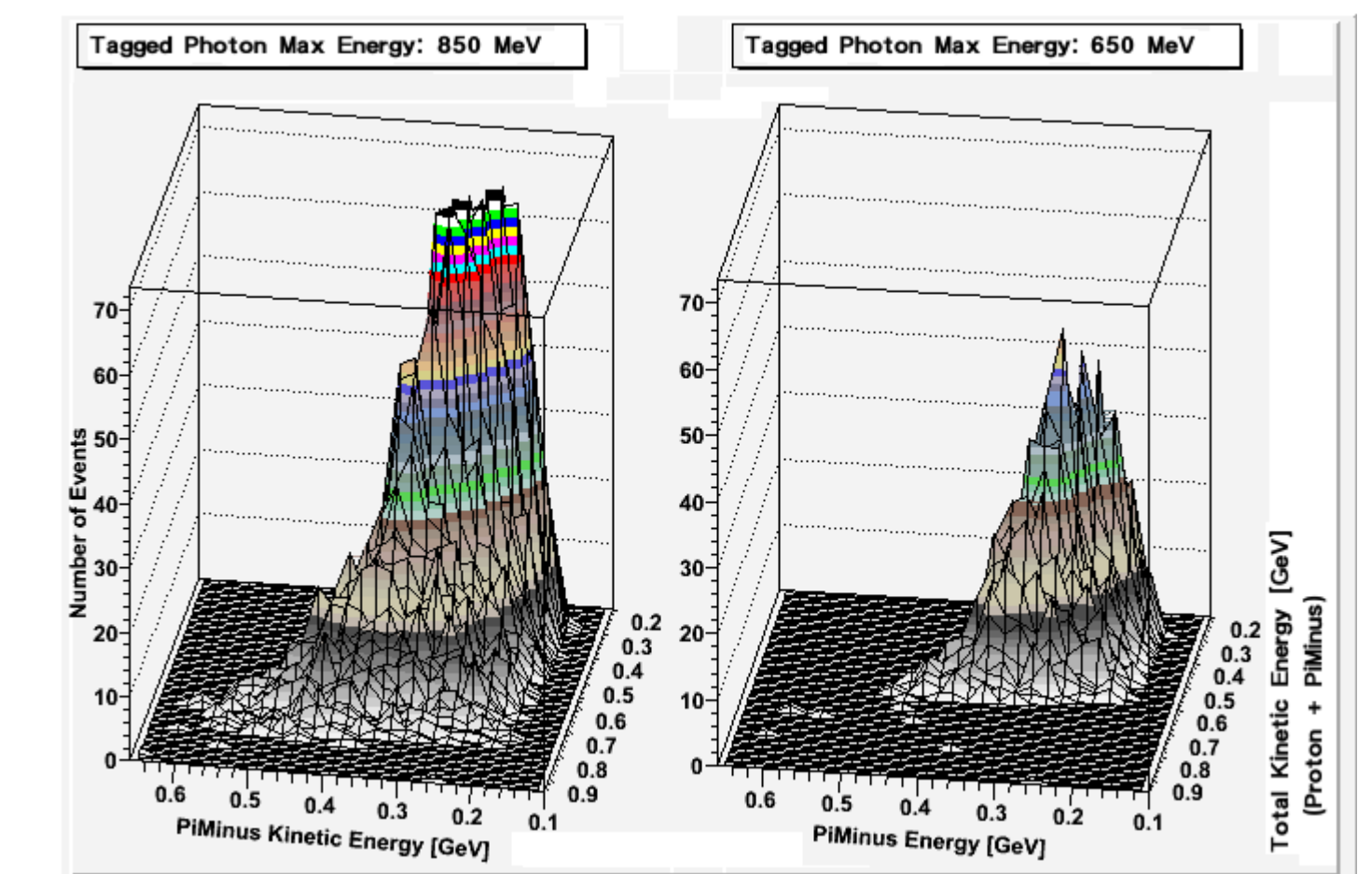


Figure 8: Two-Dimension distributions of the  $\pi^-$  kinetic energy versus the total kinetic energy.

## Summary

Using our data from CLAS, we looked at various physics distributions for signatures of eta-mesic production. However, while our data did not rule out its existence, no definitive conclusions can be made at this time.

## Future Work

While we used many different methods to try observe a signature for the eta-mesic nucleus, there are many other physics distributions to examine that can be generated from our data. We plan to continue and repeat this work for these other spectra. Also, having a theorist look at our current results would allow us to better interpret them and give us guidance for future research.

## Acknowledgments

I'd like to thank my adviser Professor Vineyard, Richie Bonventre and Christian Shultz '08 for their work and support, Union College, and the Department of Energy.

## References

- [1] L. C. Liu and Q. Haider, Phys. Rev. C **34**, 1845 (1986).
- [2] R.E. Chrien *et al.*, Phys. Rev. Lett. **60** (1988) 2595.
- [3] C. Wilkin, Phys. Rev. C **47**, R938 (1993).
- [4] M. Pfeiffer *et al.*, Phys. Rev. Lett. **92** (2001) 252001-1
- [5] V.A. Baskov *et al.*, nucl-ex/0306011v1.
- [6] G.A. Sokol *et al.*, nucl-ex/0111020v1